



# Assessing differences in the mechanical behaviour of loose cork granulates from virgin and reproduction cork

J. R. González Adrados<sup>1</sup> · J. Benito López<sup>2</sup> · C. A. Dove<sup>3</sup> · M. Sánchez-González<sup>2</sup>

Received: 13 July 2023 / Accepted: 14 February 2024 / Published online: 29 March 2024  
© The Author(s) 2024

## Abstract

Virgin cork is a little-known, sustainable and relatively scarce raw material. However, its global output is expected to increase substantially as recent cork oak plantations are stripped for the first time. The work described here aimed to examine the factors underlying the mechanical properties of granulated cork, most particularly the type of cork (virgin or reproduction), and to develop a technique to deliver fast and accurate assessments of the effects of said factors. A batch of virgin cork was boiled, dried, ground and graded following standard granule classification procedures according to size and density. The resulting granulates were then compared with equivalent commercial-grade reproduction cork granulates. Physical variables (tapped density and moisture content) were measured and elastic recovery and Young's modulus were used as proxies for mechanical properties. Image analysis was used to study the size, shape and colour of the cork particles. ANOVA results show significant effects of particle size, density class, type of cork and first and second order interactions between most variables. Density class clearly reached the highest level of significance, whereas the type of cork was less critical. A very strong correlation was found between granulates' elastic recovery and their tapped density ( $R^2=0.98$ ;  $RMSE < 1\%$ ). Likewise, greyscale imaging revealed a good adjustment between tapped density and grey level ( $R^2=0.84$ ;  $RMSE = 24 \text{ g}\cdot\text{l}^{-1}$ ). The primary conclusion was that the differences between virgin and standard cork granulates are small and should have no effect on less demanding applications. Image analysis is likely to prove useful in further, more in-depth studies.

## 1 Introduction

Forest products, as a subset of a larger group comprising all biological products, are becoming increasingly popular due to their potential to replace mineral and fossil substitutes. Forests are nowadays considered a source of renewable, biodegradable, inexpensive and abundant raw materials with great potential for developing sustainable products (Sahoo et al. 2019). In the western Mediterranean region, cork is one of such emerging sustainable forest products.

Cork is the bark of the cork oak (*Quercus suber*). It is harvested by removing the lower section of the tree's bark from the trunk in a process known as stripping. The tree grows

back its bark with no effect on its vigour or its survival. Cork is first harvested when the tree reaches a minimum circumference of 65–70 cm, i.e. at around 30–40 years of age (Fig. 1).

First-harvest cork (Fig. 2) is known as virgin cork and it is unsuitable for manufacturing stoppers (Celiège 2016). Current industrial practices establish that only reproduction cork planks harvested at third and subsequent harvests can be used to make natural and granulated stoppers (Fig. 2).

The many products and co-products obtained from cork, their value chains, the biology of the cork oak and the cork harvesting process have been described in detail (Fortes et al. 2004; Knapic et al. 2016; Pereira 2007, 2015; Silva et al. 2005).

Global cork production is underpinned by the existence of natural cork oak forests scattered across the western Mediterranean basin. However, a substantial portion of this region is devoted to agro-silvo-pastoral uses which hamper regeneration and drive trees towards an aging state. For years the decay of cork oak forests has had deleterious effects on cork productivity (Acacio et al. 2021; Cardillo et al. 2021; Vogiatzakis et al. 2020). To overcome this, over the last

✉ J. R. González Adrados  
joseramon.gonzalez.adrados@upm.es

<sup>1</sup> MONTES (ETSI de Montes, Forestal y del Medio Natural), Universidad Politécnica de Madrid (UPM), Madrid, Spain

<sup>2</sup> Institute of Forest Science (ICIFOR-INIA, CSIC), Madrid, Spain

<sup>3</sup> Systems Biology Department, National Centre for Biotechnology (CNB-CSIC), Madrid, Spain



**Fig. 1** Young cork oak with irrigation support immediately after the first stripping. The unstripped upper section of the trunk shows the original bark (virgin cork). In the lower stripped section, the tree will grow a new, more uniform bark (reproduction cork)

few decades of the twentieth century the European Union invested substantially in funding restocking of cork oak on abandoned arable farming land (Duque-Lazo et al. 2018). A more recent line of action has been to support cork oak plantations with irrigation. The resulting 10–33% growth increases in terms of trunk diameter reduce tree age at first harvest between 6 and 10 years (Alves et al. 2020; Vessella et al. 2010). Hence, a considerable affluence of virgin cork is expected in the coming years. In fact, it has been estimated that virgin cork output in the Spanish region of Extremadura will rise from 492 t in 2019 (MITECO 2020) to an average 1.630 t/year in the period ranging from 2026 to 2060 (Santiago Beltrán et al. 2022). However, granulates are the only virgin cork products currently in demand.

Reproduction cork granulates are the main co-product obtained from the manufacture of cork-stoppers. Their most traditional and value-added application is the manufacture of agglomerated cork stoppers, although only top quality granulates are suitable for this purpose.

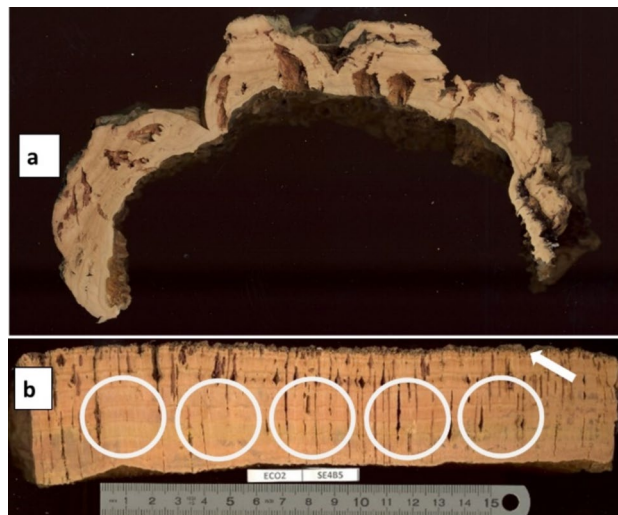


**Fig. 2** Cross-sections of cork planks. In both images, the upper layer is the outside of the tree and the lower layer is the contact area between the cork and tree trunk. **a** Virgin cork obtained from a young tree after the first stripping. **b** Reproduction cork harvested from an adult tree after several cork strippings. Circles mark the area where stoppers would be punched. The arrow marks the dry, woody tissue (back tissue) that was exposed with the previous stripping procedure

Cork granulate is a raw material with many great advantages. Not least is its minimal environmental footprint. Despite it being a topic currently under study, it can safely be stated that cork products contribute to reducing carbon footprints along their value chains (Rives et al. 2013). Process emissions are mostly attributed to the main product, i.e. natural cork stoppers, whilst co-products such as granulates account for a very small fraction (Flor-Montalvo et al. 2022). This is precisely one of the reasons behind the ever-growing number of applications for cork composites in several fields of engineering (Duarte and Bordado 2015; Gil 2015), including thermal and acoustic insulation of buildings and the manufacture of sandwich structures (Duarte and Bordado 2015; Gil 2015; Knapic et al. 2016; Sergi et al. 2022). In addition, it is important to note the growing number of applications for loose, unbound granulates, such as the manufacture of biocoals (Wang et al. 2022), bioremediation (Celeiro et al. 2020; Todescato et al. 2021), packaging (Motte et al. 2017) and as a substitute for shredded tyres as filler particles for sports fields (Armada et al. 2022; Celeiro et al. 2021; Gil 2015).

Characterisation of virgin cork granulates is required prior to their use as a substitute for reproduction cork granulates in traditional applications. Therefore, a comparative study is necessary to elucidate whether virgin cork meets the requirements to replace reproduction cork in order to satisfy the growing demand for cork granulates.

Virgin cork is different from reproduction cork in its macroscopic appearance (Fig. 2) and, to a lesser extent, in its

structure and chemical composition (Pereira 1982). However, literature on this topic is scarce and no results were found regarding the characterisation and mechanical properties of virgin cork or virgin cork granulates. Similarly, no results were found for reproduction cork granulates, except for one reference which deals with their mechanical behaviour (Motte et al. 2017).

Improving the available knowledge of virgin cork granulates should contribute to raising their market value and, therefore, their economic profitability and social awareness of recent cork oak plantations. This in itself justifies the need for a detailed study of the main properties of virgin cork granulates.

The research described here aimed to assess the effects of the type of cork (virgin or reproduction), particle size distribution and density on the mechanical properties of cork granulates. Specifically, it aimed to establish any potential differences between virgin cork and reproduction cork granulates in terms of their physical (size, shape, colour, density, moisture) and mechanical properties.

The starting hypothesis was that there are no differences between virgin cork and reproduction cork granulates, neither in terms of marketing parameters (shape and size of the particles) nor in terms of their physical (density, moisture) and mechanical (elastic recovery, Young's modulus) properties. Confirming this hypothesis whilst studying the variability of the parameters and how they might be influenced by (i) the type of cork or (ii) the industrial grading process according to particle size and density was the main target of the work. A secondary objective was to develop a methodology to support rapid characterisation of cork granulates' main physical and mechanical properties using image analysis.

## 2 Materials and methods

### 2.1 Cork granulates

Two types of loose cork granulates were used in this study: one was a standard reproduction cork granulate (RC) and the other was a virgin cork granulate (VC). 2 kg samples of the RC and VC product categories shown in Table 1 were supplied by the collaborating company Francisco Oller S.A. RC is by-product of the manufacture of single-piece natural cork stoppers. Reproduction cork planks were boiled and dried and the natural stoppers were subsequently punched out of them. All the trimmings, chips, perforated slices, etc. were collected and ground. The resulting granulates were then sifted and graded according to their density, a process that involved the removal of particles with a higher density than cork -generally woody, mineral or metallic impurities. Density grading resulted in the categories described in Table 1, which are compliant with the company's approved 0.5–2 mm size range for commercial granulates.

VC was manufactured by the collaborating company at the same facility specifically for this study. Virgin cork planks were subjected to the exact same treatment as the reproduction cork (boiling, drying, grinding) and the resulting granulates were sifted and density-graded in the same way as RC.

### 2.2 Physical properties and mechanical behaviour

Five 150 ml test specimens were collected from every sample and placed in an environmental test chamber at 20 °C and 65% relative humidity until they reached constant weight. Subsequent treatments were performed under laboratory conditions and readings for all test specimens were taken within a few minutes. Therefore, it can safely be assumed that granulate temperatures and moisture contents were kept constant.

**Table 1** Nominal characteristics of the 10 samples used in the study

| Particle size   | Product category (nominal density range)          | Type of cork | Sample code |
|-----------------|---|--------------|-------------|
| Coarse (1–2 mm) | High density (220–250 g·l <sup>-1</sup> )         | Reproduction | RCH         |
|                 |   | Virgin       | VCH         |
|                 | Intermediate density (100–120 g·l <sup>-1</sup> ) | Reproduction | RCI         |
|                 |   | Virgin       | VCI         |
|                 | Low density (58–62 g·l <sup>-1</sup> )            | Reproduction | RCL         |
|                 |   | Virgin       | VCL         |
| Fine (0.5–1 mm) | Intermediate density (100–120 g·l <sup>-1</sup> ) | Reproduction | RFI         |
|                 |   | Virgin       | VFI         |
|                 | Low density (58–62 g·l <sup>-1</sup> )            | Reproduction | RFL         |
|                 |   | Virgin       | VFL         |

Tapped volume was measured by filling a metal vessel ( $\varnothing=5\text{cm}$ ;  $h=6,1\text{cm}$ ) to the brim with each of the test specimens and placing it on an orbital shaker set to 270 rpm for 60 s. Tapped density (D60) was calculated as the ratio of the mass of granulate in the vessel to its tapped volume:

$$D60 = M/V_p \quad (1)$$

where  $M$  is mass in grams and  $V_p$  is tapped volume in litres.

At the end of every assay, granulate moisture content ( $H$ ) was measured as the difference in weight before and after drying in a heat chamber at  $103^\circ\text{C}$ .

Mechanical properties were analysed using a similar methodology to that of previously published works (Motte et al. 2017). Simple uniaxial compression tests were carried out using a ZwickRoell Z020 testing machine (Zwick GmbH & Co., KG, Ulm, Germany) (Supplementary material, Fig. SM1). For each of the test specimens, the metal vessel filled with granulate was placed under the moving crosshead of the testing machine, progressively loaded at  $3.5\text{ N s}^{-1}$  up to  $\sigma=380\text{ kPa}$  and then immediately unloaded. Elastic recovery was calculated using Armstrong and Haines-Nutt's equation (Motte et al. 2017) for powder bed compaction:

$$ER = (h - h_p)/h \quad (2)$$

where  $h_p$  and  $h$  are the thickness of the packed granulate at confining stress and 500 s after unloading the test specimen.

Stress–strain curves were plotted for all granulate samples (Fig. 3) and Young's modulus calculated for each curve as the slope of its linear elastic portion, i.e. between 1 and 2%

strain values (Fortes et al. 2004). Values of Young's modulus were considered valid when the percentage of variability explained was at least 99% and the slope was significantly different from zero.

### 2.3 Particle image analysis

The image analysis methodology described in previously published works (Motte et al. 2017; Vaezi et al. 2013) was used in this study with the addition of colour measurement by means of greyscale imaging. Five RGB images were obtained for each sample by scattering granulate particles on the surface of a commercial HP Scanjet G4010 scanner in such a way that they were sufficiently apart from each other. Image resolution was set to 600 dpi to capture between 250 and 2000 particles per image depending on particle size. ImageJ software (Abràmoff et al. 2004) and the “analyze images” plugin were used to transform scanned images into 16-bit type images (greyscale) and measure the size (area and maximum caliper -Ferret diameter-), shape and colour (grey level) of every particle.

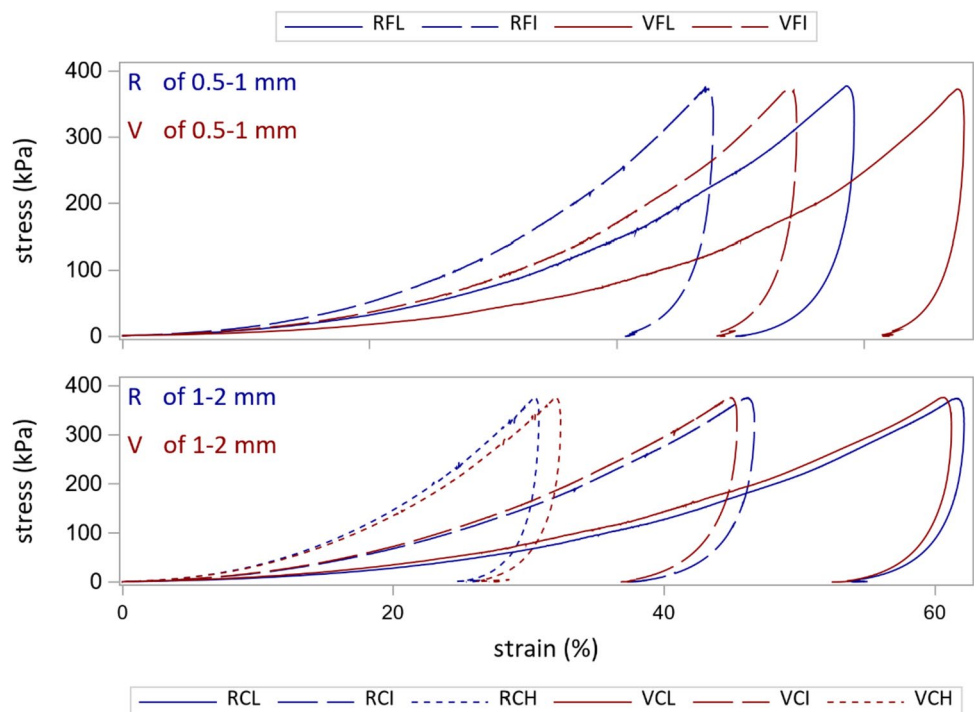
The following shape parameters were considered:

– Circularity ( $C$ ) which is a function of the perimeter ( $P$ ) and the area ( $A$ ) of the particle:

$$C = (4 * \pi * A)/P^2 \quad (3)$$

Values of  $C$  range between 0 and 1 ( $0 < C \leq 1$ ). 1 indicates a perfect circle, whereas 0 would be an infinitely elongated shape.

**Fig. 3** Average stress–strain curves for fine (up) and coarse (down) samples. Codes refer to type of cork (R: reproduction cork; V: virgin cork), particle sizes (C: coarse, F: fine), product categories (H: high, I: intermediate, L: Low) (see Table 1)



– Aspect ratio (AR):

$$AR = a/b \quad (AR > 1) \quad (4)$$

where *a* and *b* are respectively the major and minor axes of the ellipse that best fits the particle.

– Solidity (S):

$$S = A/F \quad (0 < S \leq 1) \quad (5)$$

where *F* is the convex hull of the particle, which can be pictured as a rubber band wrapped tightly around the points that define the particle. Solidity indicates the degree of convexity of the particle. For a perfectly convex particle  $S = 1$ .

Particle colour was measured as the mode of the shades of grey (grey level) displayed by all pixels within the contour of a single particle.

Homogeneity of particle size distribution and shape and colour variables were measured using Vaezzi's uniformity index (Vaezi et al. 2013):

$$UI = (P5/P90) * 100 \quad (6)$$

where *P5* and *P90* are the values of percentiles 5% and 90% for each variable.

## 2.4 Statistical analysis

Mean and standard deviation for each of the measured variables, as well as minimum and maximum values were calculated (Supplementary material, Table SM1 and Table SM2). In a preliminary analysis, graphs were used to test all data for linearity, homogeneity of variance and normality. Standardised residuals for all models were plotted against independent variables to detect heterogeneity or trends in variance. If assumptions on normality and homogeneity of variance were not met, Kruskal–Wallis non-parametric tests and post hoc Dunn's tests were performed to adjust for multiple pairwise comparisons across the ten sample types using the SAS macro developed by Elliott and Hynan (2011). Otherwise, each of the physical and mechanical variables, i.e. tapped density, moisture content, elastic recovery and Young's modulus, together with circularity and grey level, were also analysed using a three-way ANOVA where type of cork, particle size and product category were the main effects and all their possible interactions were considered. No transformation of data was required to meet ANOVA assumptions. Significant differences in means were tested amongst groups by comparing estimated marginal means with Tukey adjustments for multiple comparisons. In addition, the Pearson correlation coefficient and linear regression analyses were used to assess the relationships between variables. All tests were conducted at the  $\alpha = 0.05$  level using SAS software version 9.4 (SAS Institute Inc. 2016).

## 3 Results

### 3.1 Physical properties and mechanical behaviour

Table SM1 (Supplementary material) summarises the main results obtained for the studied variables. Tapped density was mostly within the set limits for each of the product categories. Low density granulates were the sole exception, with mean values ranging from 61.3 to 77.7  $\text{g}\cdot\text{l}^{-1}$ , i.e. in most cases slightly above nominal limits (58–62  $\text{g}\cdot\text{l}^{-1}$ ). Mean moisture content for high and intermediate product categories ranged from 7.73 to 13.58%. These latter figures were relatively high compared to data found in the literature for similar product categories. It has been reported that under the conditions set in this study (20 °C, 65% RH), cork without woody inclusions stabilises at an equilibrium moisture content between 6 and 7% (González-Adrados et al. 2012; Lequin et al. 2010).

Stress–strain curves (Fig. 3) illustrate the mechanical behaviour of cork granulate samples tested for simple compression. Curves were shaped differently and Young's modulus values were much lower compared to previous studies with 20 mm-edge natural cork cubes (Anjos et al. 2014; Fortes et al. 2004). At fixed loads, lower density granulates (RFL, VFL, RCL, VCL) registered deformation values above 50%, whilst deformation hardly reached 30% for high-density granulates (RCH, VCH). These deformation values set the upper and lower limits for the remaining granulates.

Physical and mechanical variables (tapped density, moisture content, elastic recovery and Young's modulus) met normality and homogeneity of variance assumptions. Therefore, data were analysed by means of a three-way ANOVA using type of cork, particle size and product category as the main effects and considering all of their possible interactions. No transformation of data was required to meet ANOVA assumptions. The three-way interaction type of cork\*particle size\*product category was significant ( $P < 0.001$ ) for the four variables tested (Table 2). The presence of this significant second-order interaction suggests that it is not easy to draw clear conclusions from the study of the main effects and their first order interactions, significant or otherwise. To analyse this three-way interaction, the type of cork\*particle size interaction for all product categories and the type of cork\*product category interaction at all particle sizes were plotted for the four tested variables (Supplementary material: tapped density (Fig. SM2), moisture content (Fig. SM3), elastic recovery (Fig. SM4) and Young's modulus (Fig. SM5)).

ANOVA results and Figures SM2 to SM5 reflect how empirical-knowledge-based commercial size and density grading affect physical and mechanical variables; the effect

**Table 2** Three-way ANOVA to test the effects of the type of cork, particle size, product category and their interactions on physical and mechanical variables

| Effect                | Df | D60       | H         | ER        | E       | Circ     | Grey      |
|-----------------------|----|-----------|-----------|-----------|---------|----------|-----------|
| Type of cork (ToC)    | 1  | 233.7***  | 758.5***  | 120.8***  | 0.4     | 91.3***  | 57.8***   |
| Particle size (PS)    | 1  | 0.05      | 130.6***  | 1.5       | 17.5*** | 830.3*** | 65.0***   |
| ToC*PS                | 1  | 233.6***  | 0.0       | 200.2***  | 11.0*** | 105.0*** | 127.7***  |
| Product category (PC) | 2  | 8579.0*** | 6982.8*** | 2079.9*** | 61.4*** | 954.4*** | 1997.9*** |
| ToC*PC                | 2  | 89.5***   | 138.0***  | 10.9***   | 0.2     | 9.4***   | 48.7***   |
| PS*PC                 | 1  | 0.9       | 448.6***  | 0.1       | 0.0     | 695.5*** | 251.3***  |
| ToC*PS*PC             | 1  | 26.8***   | 138.4***  | 21.1***   | 0.0     | 13.27*** | 48.2***   |

D60 is tapped density, H is moisture content, ER is elastic recovery, E is the Young's modulus, Circ is circularity and Grey is the median grey level

Df is the degree of freedom and all other figures are the F value. \*, \*\*, and \*\*\* are the significance level at  $P < 0.05$ ,  $0.01$ , and  $0.001$ , respectively

**Table 3** Pearsons' correlation coefficient between physical and mechanical variables and between the latter and grey level ( $P < 0.001$  in all cases)

| Variable | D60    | H      | ER     | E      |
|----------|--------|--------|--------|--------|
| H        | 0.952  |        |        |        |
| ER       | -0.920 | -0.924 |        |        |
| E        | 0.945  | 0.867  | -0.916 |        |
| grey     | -0.918 | -0.970 | 0.888  | -0.832 |

of the type of cork, although significant, is much smaller in all cases. This statement is best illustrated by (i) the expected influence of product-category-controlled density (Fig. SM2 right) on other variables such as H (Fig. SM3, right) and ER (Fig. SM4, right) and (ii) the effect that the type of cork had on some variables, such as H, despite the overriding influence of density. Note that virgin cork's moisture content was lower than reproduction cork's for most of the factor combinations (Fig. SM3).

Correlation analysis was done using an average-value matrix ( $n = 10$ ) for the main variables (physical, mechanical and image analysis) (Table 3). Results show a strong correlation between physical and mechanical properties. This becomes particularly clear in the case of tapped density (D60), which is directly proportional to moisture content and Young's modulus and inversely proportional to elastic recovery.

### 3.2 Particle image analysis

Average values for particle size, shape and colour, as well as a detailed description of size distribution for each sample can be found in the supplementary material (Table SM2, Fig. SM6). Four out of six variables used in the image analyses (FeretMax, area, solidity and aspect ratio) did not meet normality and heteroscedasticity assumptions. Therefore, in addition to a descriptive analysis, a Kruskal–Wallis test was

performed to assess the differences between the ten sample types. Although a significant effect of the sample factor was found for all sample types at a significance level below 0.01%, the differences were one-off and very small. This led to the conclusion that no notable differences were found between the virgin and reproduction cork granulates with regards to these variables.

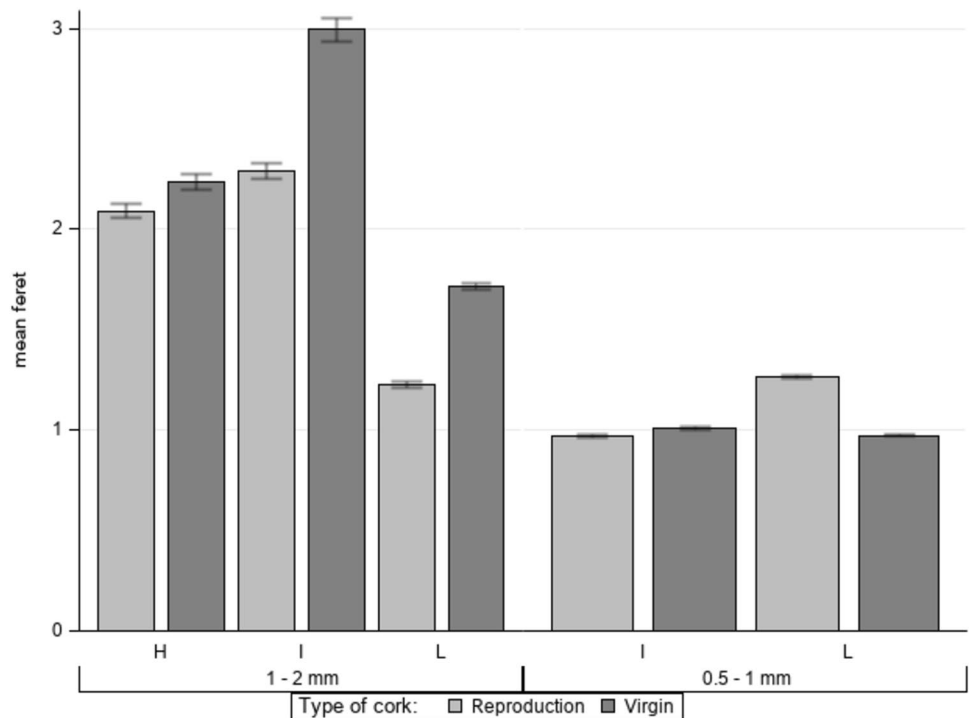
Mean grey level and circularity did meet normality and heteroscedasticity assumptions and, therefore, could be analysed with the three-way ANOVA used previously (Table 2). The three-way interaction cork type\*particle size\*product category was significant for both variables ( $P = 0.0003$  and  $P < 0.001$ , respectively) (Table 2) and was analysed in the same way as the mechanical variables (Figs. SM7 and SM8).

Maximum particle diameter (FeretMax) was studied in detail (Fig. 4, Fig. SM6) because particle sizes were often larger than the sieve openings used in the sifting phase, e.g. FeretMax  $> 2$  mm for most of the coarse samples. This anomaly was also observed by preceding authors and is caused by elongated particles that are able to pass through the mesh screen and subsequently rest on their larger sides on the scanner. Because image analysis software typically considers particles' two larger dimensions, it tends to overestimate the size of these elongated particles.

Homogeneity of particle size distribution measured with the uniformity index (UI) varied notably amongst samples (Table SM2). Fine granulates displayed peak values of UI ( $UI_{\text{FeretMax}} = 48.86$ ,  $UI_{\text{Area}} = 28.09$ ) whilst coarse granulates registered smaller values ( $UI_{\text{FeretMax}} = 26.44$ ,  $UI_{\text{Area}} = 7.50$ ). This is a result of the sifting process, i.e. smaller particles can sometimes be retained by sieves with a larger mesh opening (1 mm), but it is not possible for larger particles to pass through smaller mesh sizes.

Regarding shape, results matched expectations and were similar to previously published figures (Table SM2): (i) elongated particles with a length-to-width ratio between 1.5 and 2 ( $AR = 1.5-2$ ), (ii) moderately spherical particles (average circularity values between 0.47 and 0.62) and (iii)

**Fig. 4** Mean maximum particle diameter (FeretMax) values for coarse (left) and fine (Right) samples (mm). Letters at the base of each pair of columns indicate the product category: high density (H), intermediate density (I), low density (L)



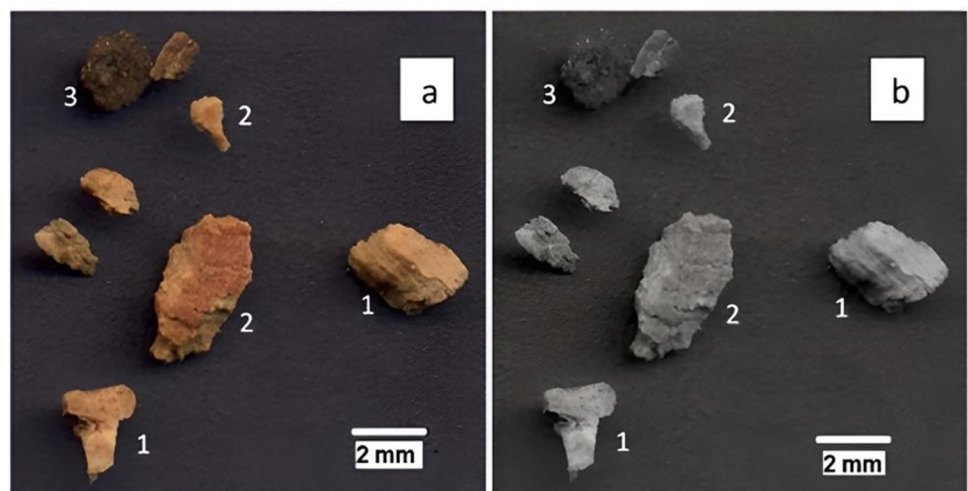
clearly convex particles (average solidity values between 0.81 y 0.86) similar to those described in previous works ( $0.89 \pm 0.04$ ) (Motte et al. 2017). This suggests that milling processes are quite uniform across the European cork industry. Differences in circularity between virgin and reproduction cork were almost non-existent for coarse samples (1–2 mm) and small in the case of fine samples (Fig. SM7).

Finally, particle colour in terms of grey level was quite homogeneous across all samples ( $UI = 59.86\text{--}65.10$ ), with average values clearly driven by product category. Irrespective of particle size, product categories with higher nominal densities (H, I) registered lower grey level values, i.e. darker

colour, whilst product categories with lower nominal densities (L) returned higher grey level values (lighter colour). The explanation for this is that, as seen at microscopic scale (Pereira 2007) (p. 40 ff), denser tissues present in the granule (lignified areas, summer-autumn cells which are smaller in size and have thicker walls, anomalies like “earthy” cork) have a darker colour, whilst lighter areas are made up of larger spring–summer cells with thinner walls (Fig. 5).

Granules from defect-free areas of the plank where the only tissue present was cork had a lower density. On the contrary, the presence of any other type of tissue or areas with higher density summer-autumn cork cells would result in

**Fig. 5** RGB (a) and 16-bit (grey scale) (b) image of granules from RCH sample (coarse, high density reproduction cork). 1: pure cork granules; darker zones correspond to summer-autumn cells. 2: granules with anomalies (“earthy” tissue). 3: granules with woody back tissue



higher density granules (Fortes et al. 2004). Most virgin cork samples had a lighter colour than reproduction cork samples, which suggests that the type of cork had some effect on the grey level variable (Fig. SM8).

Correlation results (Table 3) show that the median grey level displayed a significantly strong correlation ( $p < 0.001$  in all cases) with physical and mechanical variables: tapped density (Pearson's correlation coefficient = -0.918), moisture content (Pearson's correlation coefficient = -0.970), elastic recovery (Pearson's correlation coefficient = 0.888,) and Young's modulus (Pearson's correlation coefficient = -0.832).

## 4 Discussion

As is the case with all forest products where genetic intervention has been kept low or is non-existent, the characteristics of cork vary to a high degree. This work aimed to deliver new knowledge about the physical and mechanical properties of cork by studying the variability of virgin cork granulates, a raw material which until now had been scarcely studied.

Variance analysis (Table 2) shows the influence that the factors considered (type of cork, particle size, product category) had over the physical and mechanical properties of granulates, as well as the existence of interactions between them. Despite this hampering easy interpretation of the results, a very high level of significance was found for the influence of Product Category on Density (D60) -which is obvious- but also on Moisture Content (H) and mechanical performance (ER, E). This suggests that granulate manufacturers are empirically aware of the critical effect of density, which most likely is why they use this parameter to grade cork granulates into product categories. Despite the difficulties encountered with the interpretation of results, it stood out that for most variables the F value was much greater for the product category factor than for all other factors and their interactions.

The variables behind cork's mechanical performance have been studied in depth since the initial works on the subject were published towards the end of the twentieth century (Fortes et al. 2004; Gibson et al. 1981). Specifically, compressive stiffness was found to be closely related to density in 20 mm-edge natural cork cubes (Anjos et al. 2014) and agglomerated cork products. Compressive stiffness was also found to be directly proportional to particle size in agglomerated cork (Sergi et al. 2022). Figure 3 shows that loose granulates behaved in exactly the same way: under constant strain, deformation was greater at lower densities and particle sizes. Quite conspicuous significant differences were found between the curves of fine granulates, but not between the curves of their coarse counterparts. Regardless of particle size, compressive stiffness was lower for virgin

cork granulates (VFL, VFI) than for reproduction cork granulates (RFL, RFI).

Relationships between tapped density (D60), elastic recovery (ER), moisture content (H) and colour are due to the variability in the composition of tissues present in granules. As explained above, darker colour is related to the presence of denser woody tissues and anomalies, which do not have the elastic properties of pure cork cells. This also explains why H was found to be greater in dense granulates and, to a lesser extent, why it was higher in reproduction cork compared to virgin cork. Water molecules attach to free OH radicals, which are abundant in woody materials and scarce in the very hydrophobic suberin, the main component of cork cells. The type-of-cork effect would be contained already in the density effect: virgin cork does not incorporate most of the woody inclusions present in reproduction cork (back tissue) and is therefore slightly less dense than reproduction cork. This is the reason for its relatively greater elastic recovery and lower moisture content.

Strong correlations found between, on the one hand, elastic recovery and density and, on the other hand, grey level and tapped density encouraged the development of a model to describe the relationships between variables. Several models were tested to describe the relationship between tapped density and elastic recovery and the reverse model delivered the best results. Figure 6 shows a scatterplot of elastic recovery against tapped density and the corresponding regression curve. The regression equation was:

$$ER = 4.05 + (2033.46/D60) \quad (7)$$

where ER is elastic recovery in % and D60 is tapped density in  $\text{g}\cdot\text{l}^{-1}$ . This regression model accounts for over 98% of the variance and predicts elastic recovery to a high (0.9560) degree of accuracy (RMSE). Graphical analysis of the residuals showed that they were randomly distributed without a clear pattern (Fig. SM9).

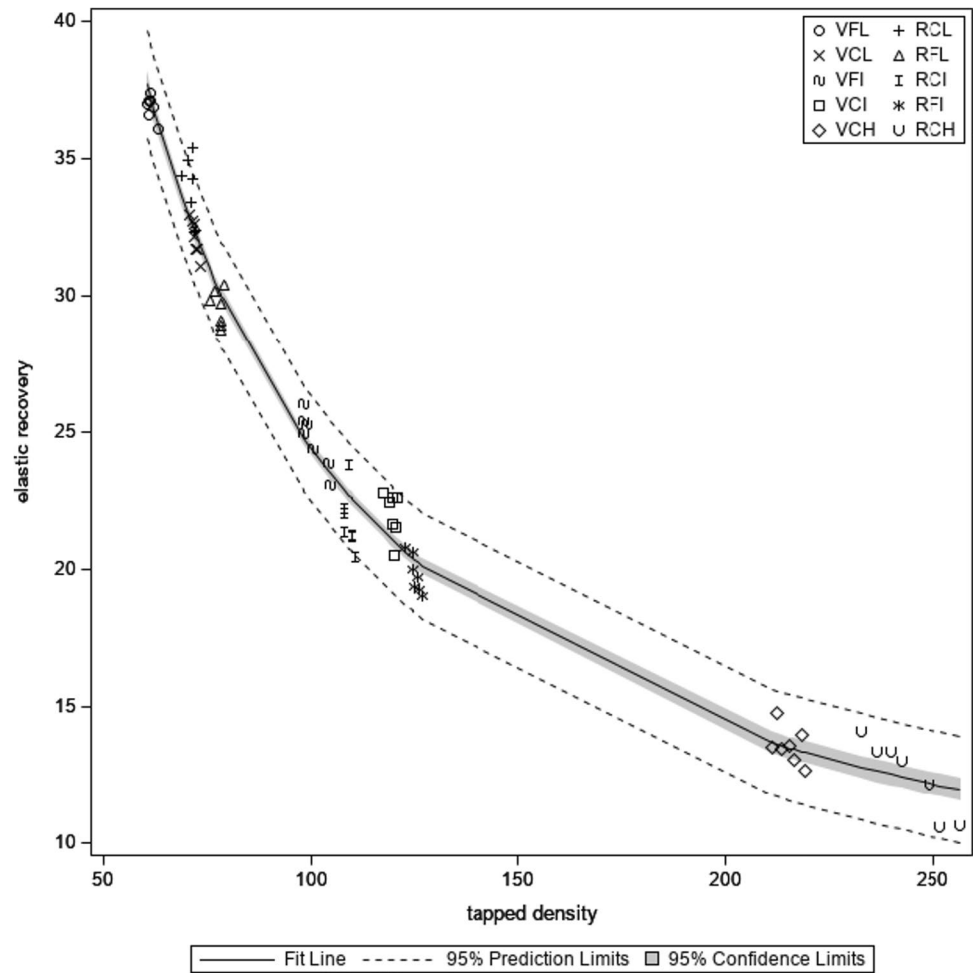
This shows that mechanical performance of cork granulates is driven almost exclusively by density. The greater the density, the greater the compression stiffness and the lower the elastic recovery.

Correlations found in the mean value matrix ( $n = 10$ ) (Table 3) suggest that it is possible to estimate the main variables with grey level readings. The relationship between tapped density and grey level also returned a high level of significance using a simple linear model ( $R^2 = 0.840$ ) (Fig. 7 left). The regression equation was:

$$D60 = 914.116 - 6.58 * \text{grey} \quad (8)$$

where D60 is tapped density in  $\text{g}\cdot\text{l}^{-1}$  and grey is the median grey level. This model predicts tapped density with a  $24.0 \text{ g}\cdot\text{l}^{-1}$  accuracy (RMSE).

**Fig. 6** Tapped density ( $\text{g}\cdot\text{l}^{-1}$ ) vs elastic recovery (%) scatterplot. The solid line is the regression line (Eq. 7). The dark-shaded region shows the 95% confidence interval and dashed lines are the regression's upper and lower 95% prediction intervals. The symbol of the data points refers to the sample type (see Table 1)



An exponential model also returned a good level of significance ( $R^2=0.8856$ ) for the relationship between ER and grey level. The regression equation in this case was (Fig. 7, right):

$$ER = 0.308 * e^{0.036\text{grey}} \tag{9}$$

where ER is elastic recovery in % and grey is the median grey level. This regression model predicts elastic recovery with a 3.8% accuracy (RMSE).

Graphical analysis of the residuals showed that they are randomly distributed without a clear pattern (Fig. SM10).

These models support accurate estimation of a granulate's density and mechanical performance using simple image analysis. More complex techniques such as NIRS (Perez-Terrazas et al. 2020) are likely to make relevant contributions towards a full characterisation of cork granulates.

### 5 Conclusion

Cork granulates, like most forest products, remain heterogeneous in terms of their physical and mechanical properties even after undergoing processes designed to reduce such

heterogeneity (sifting, product grading according to density and stabilisation in an environmental test chamber).

Type of cork (reproduction cork or virgin cork) has a significant effect on cork granulates' physical properties and mechanical performance. However, such an effect is driven by other factors that came into play in this study (particle size, product category). In fact, product categorisation based on granulate density was found to be the critical factor.

Mechanical response to uniaxial compression in terms of elastic recovery is mostly dependent on tapped density. Regardless of the combination of ruling factors it is possible to predict the level of elastic recovery of a sample of cork granulate with its tapped density. The model provided (Eq. 7) predicts elastic recovery with a root mean square error below 1%.

Image analysis is a fast and simple technique supporting reliable predictions of the main physical characteristics (size, shape, density) of cork granules and it may prove useful in monitoring the processes involved in the manufacture of cork granulates. A good understanding of said characteristics unlocks high-precision predictions of cork granulates' mechanical performance under compression.

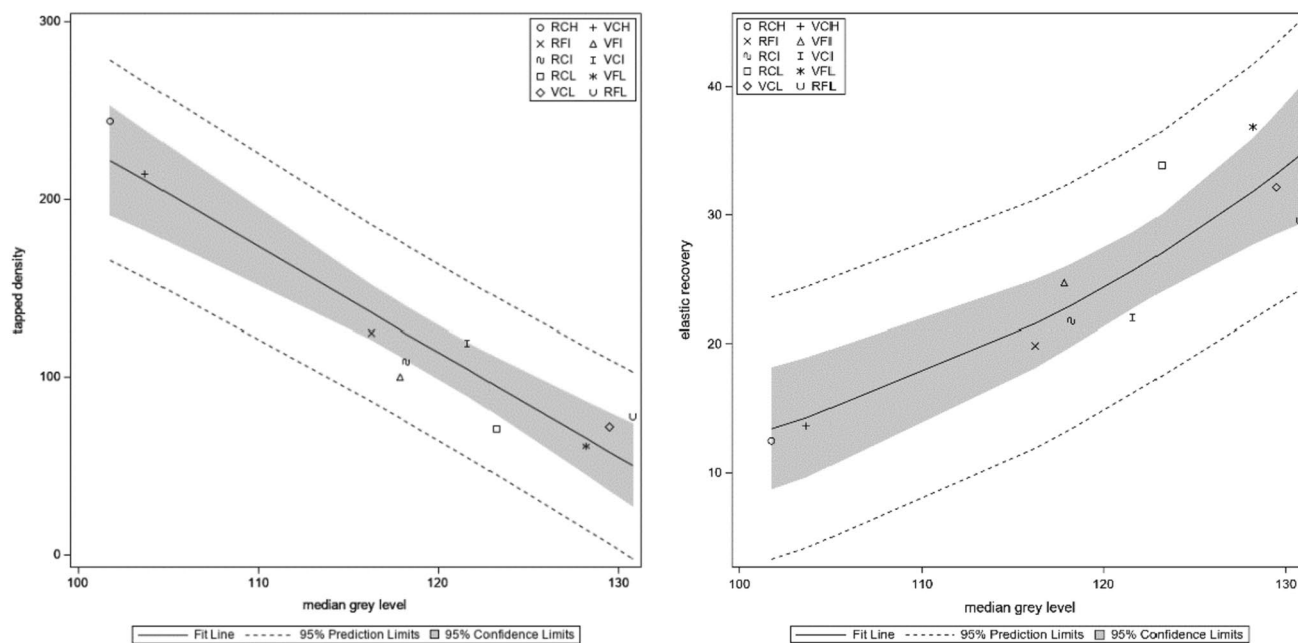


**Fig. 7** Left: grey level (average-value matrix,  $n=10$ ) vs tapped density ( $\text{g l}^{-1}$ ) scatterplot. The solid line is the regression line (Eq. 8). The dark-shaded region shows the 95% confidence interval and dashed lines are the upper and lower 95% prediction intervals of

the regression. Sample codes as shown in Table 1. Right: grey level (average-value matrix,  $n=10$ ) vs elastic recovery (%) scatterplot (Eq. 9)

The differences in mechanical performance between virgin and reproduction cork granulates are small and should have no effect in applications where granulates do not need to be bound, e.g. sports field infilling. However, further research is needed regarding other applications, such as composite manufacturing.

**Supplementary Information** The online version contains supplementary material available at <https://doi.org/10.1007/s00107-024-02057-3>.

**Acknowledgements** The authors would like to thank Francisco Oller S.A. for providing the material for this work and for advising on the cork granulate production process. Authors also acknowledge the detailed analysis and comments received from the two anonymous reviewers. This work is part of the R&D project RTI2018-094413-R-C21. BIOBOR Bornizo para la Bioeconomía: Herramientas de gestión forestal y evaluación ambiental para su valorización [Tools for forest management and environmental assessment for the valorization of virgin cork] funded by MCIN/736 AEI/<https://doi.org/10.13039/501100011033/>

**Author contributions** Jose R. Gonzalez Adrados: Conceptualization, Methodology, Literature Review, Writing—original draft, Writing—review & editing. Jorge Benito Lopez: Methodology, Investigation, Data curation. Mariola Sanchez Gonzalez: Conceptualization, Formal analysis, Investigation, Writing—original draft. Clive A. Dove: Writing—original draft, Writing—review & editing.

**Funding** Open Access funding provided thanks to the CRUE-CSIC agreement with Springer Nature.

**Data availability** Data are available under request to corresponding author.

## Declarations

**Conflict of interest** The authors declare no competing interests.

**Open Access** This article is licensed under a Creative Commons Attribution 4.0 International License, which permits use, sharing, adaptation, distribution and reproduction in any medium or format, as long as you give appropriate credit to the original author(s) and the source, provide a link to the Creative Commons licence, and indicate if changes were made. The images or other third party material in this article are included in the article's Creative Commons licence, unless indicated otherwise in a credit line to the material. If material is not included in the article's Creative Commons licence and your intended use is not permitted by statutory regulation or exceeds the permitted use, you will need to obtain permission directly from the copyright holder. To view a copy of this licence, visit <http://creativecommons.org/licenses/by/4.0/>.

## References

- Abràmoff MD, Magalhães PJ, Ram SJ (2004) Image processing with ImageJ. *Biophoton Int* 11:36–42
- Acacio V, Dias FS, Catry FX, Bugalho MN, Moreira F (2021) Canopy cover loss of Mediterranean oak woodlands: long-term effects of management and climate. *Ecosystems* 24:1775–1791. <https://doi.org/10.1007/s10021-021-00617-9>

- Alves CC, Dinis C, Vaz M, Barroso JM, Ribeiro NA (2020) Irrigation of young cork oaks under field conditions—testing the best water volume. *Forests* 11:88. <https://doi.org/10.3390/f11010088>
- Anjos O, Rodrigues C, Morais J, Pereira H (2014) Effect of density on the compression behaviour of cork. *Mater Des* 53:1089–1096. <https://doi.org/10.1016/j.matdes.2013.07.038>
- Armada D, Llompert M, Celeiro M, Garcia-Castro P, Ratola N, Dagnac T, de Boer J (2022) Global evaluation of the chemical hazard of recycled tire crumb rubber employed on worldwide synthetic turf football pitches. *Sci Total Environ* 812:152542. <https://doi.org/10.1016/j.scitotenv.2021.152542>
- Cardillo E, Abad E, Meyer S (2021) Iberian oak decline caused by *Phytophthora cinnamomi*: a spatiotemporal analysis incorporating the effect of host heterogeneities at landscape scale. *For Pathol* 51:e12667. <https://doi.org/10.1111/efp.12667>
- Celeiro M, Vazquez L, Sergazina M, Docampo S, Dagnac T, Vilar VJP, Llompert M (2020) Turning cork by-products into smart and green materials for solid-phase extraction-gas chromatography tandem mass spectrometry analysis of fungicides in water. *J Chromatogr A* 1628:461437. <https://doi.org/10.1016/j.chroma.2020.461437>
- Celeiro M, Armada D, Dagnac T, de Boer J, Llompert M (2021) Hazardous compounds in recreational and urban recycled surfaces made from crumb rubber. Compliance with current regulation and future perspectives. *Sci Total Environ* 755:142566. <https://doi.org/10.1016/j.scitotenv.2020.142566>
- Celiège (2016) International Code of Cork Stopper Manufacturing Practice. [https://celiege.eu/systecode\\_](https://celiege.eu/systecode_). Accessed 20 Sep 2022
- Duarte AP, Bordado JC (2015) Cork—a renewable raw material: forecast of industrial potential and development priorities. *Front Mater* 2:2. <https://doi.org/10.3389/fmats.2015.00002>
- Duque-Lazo J, Navarro-Cerrillo RM, Ruiz-Gomez FJ (2018) Assessment of the future stability of cork oak (*Quercus suber* L.) afforestation under climate change scenarios in Southwest Spain. *For Ecol Manage* 409:444–456. <https://doi.org/10.1016/j.foreco.2017.11.042>
- Elliott AC, Hynan LS (2011) A SAS (R) macro implementation of a multiple comparison post hoc test for a Kruskal-Wallis analysis. *Comput Methods Programs Biomed* 102:75–80. <https://doi.org/10.1016/j.cmpb.2010.11.002>
- Flor-Montalvo F, Martínez-Camara E, Luis García-Alcaraz J, Jiménez-Macias E, Latorre-Biel J, Blanco-Fernández J (2022) Environmental impact analysis of natural cork stopper manufacturing. *Agriculture-Basel* 12:636. <https://doi.org/10.3390/agriculture12050636>
- Fortes MA, Rosa ME, Pereira H (2004) A Cortiça. IST Press, Lisboa
- Gibson LJ, Easterling KE, Ashby MF (1981) The structure and mechanics of cork. *Proceedings of the Royal Society of London. A. Mathematical and Physical Sciences*, 377(1769) pp 99–117
- Gil L (2015) New cork-based materials and applications. *Materials* 8:625–637. <https://doi.org/10.3390/ma8020625>
- González-Adrados JR, González-Hernández F, Fernández-Golfín JJ, García de CV, Conde García M, García Fernández F (2012) Electrical resistance vs moisture content in four different types of cork products. In: Davim P (ed), *Wood and Wood Products*. Nova Science Publishers, New York, pp 109
- Knapic S, Oliveira V, Machado JS, Pereira H (2016) Cork as a building material: a review. *Eur J Wood Prod* 74:775–791. <https://doi.org/10.1007/s00107-016-1076-4>
- Lequin S, Chassagne D, Karbowiak T, Gougeon R, Brachais L, Bellat JP (2010) Adsorption equilibria of water vapor on cork. *J Agric Food Chem* 58:3438–3445. <https://doi.org/10.1021/jf9039364>
- MITECO (2020) Otros aprovechamientos forestales. Datos desglosados de 2019 (Other forest harvesting. Breakdown of data for 2019). [https://www.miteco.gob.es/es/biodiversidad/estadisticas/2019\\_otros\\_aprovechamientos.aspx](https://www.miteco.gob.es/es/biodiversidad/estadisticas/2019_otros_aprovechamientos.aspx). Accessed 19 Nov 2022
- Motte J, Delenne J, Barron C, Dubreucq É, Mayer-Laigle C (2017) Elastic properties of packing of granulated cork: effect of particle size. *Ind Crop Prod* 99:126–134. <https://doi.org/10.1016/j.indcrop.2017.01.043>
- Pereira H (1982) Studies on the chemical composition of virgin and reproduction cork of *Quercus suber* L. *Anais do Instituto Superior de Agronomia*, 40:17–25
- Pereira H (2007) *Cork: biology, production and uses*. Elsevier, Oxford
- Pereira H (2015) The rationale behind cork properties: a review of structure and chemistry. *BioResources* 10:6207–6229
- Perez-Terrazas D, Gonzalez-Adrados JR, Sanchez-Gonzalez M (2020) Qualitative and quantitative assessment of cork anomalies using near infrared spectroscopy (NIRS) 24:100490. <https://doi.org/10.1016/j.fpsl.2020.100490>
- Rives J, Fernandez-Rodriguez I, Rieradevall J, Gabarrell X (2013) Integrated environmental analysis of the main cork products in southern Europe (Catalonia - Spain). *J Clean Prod* 51:289–298. <https://doi.org/10.1016/j.jclepro.2013.01.015>
- Sahoo K, Bergman R, Alanya-Rosenbaum S, Gu H, Liang S (2019) Life cycle assessment of forest-based products: a review 11:4722. <https://doi.org/10.3390/su11174722>
- Santiago Beltrán R, Lanzo Palacios R, Berdón Berdón J, Cardillo Amo E, Murillo vilanova M, Montero Calvo AJ, Fernandez Santos AM, Maya Blanco V (2022) Estudio de las repoblaciones de alcornoque en Extremadura y estimación de su producción futura de corcho (*Study of cork oak repopulations in Extremadura and estimation of future cork production*). In: SECF (ed) *Actas 8º Congreso Forestal Español, Sociedad Española de Ciencias Forestales*
- SAS Institute Inc (2016) *SAS/STAT® 14.2 User's Guide*. Cary NC., EUA
- Sergi C, Sarasini F, Tirillo J (2022) The Compressive Behavior And Crashworthiness Of Cork: A Review. *Polymers* 14:134. <https://doi.org/10.3390/polym14010134>
- Silva SP, Sabino MA, Fernandes EM, Correlo VM, Boesel LF, Reis RL (2005) Cork: properties, capabilities and applications. *Int Mater Rev* 50:345–365. <https://doi.org/10.1179/174328005X41168>
- Todescato D, Mayer DA, Cechinel MAP, Hackbarth FV, Souza AAUd, Souza SMA, de Guelli U, Vilar VJP (2021) Cork granules as electron donor in integrated reduction/oxidation and sorption processes for hexavalent chromium removal from synthetic aqueous solution. *J Environ Chem Eng* 9:105001. <https://doi.org/10.1016/j.jece.2020.105001>
- Vaezi M, Pandey V, Kumar A, Bhattacharyya S (2013) Lignocellulosic biomass particle shape and size distribution analysis using digital image processing for pipeline hydro-transportation. *Biosyst Eng* 114:97–112. <https://doi.org/10.1016/j.biosystemseng.2012.11.007>
- Vessella F, Parlante A, Schirone A, Sandoletti G, Bellarosa R, Piovesan G, Santi L, Schirone B (2010) Irrigation regime as a key factor to improve growth performance of *Quercus suber* L. *Scand J for Res* 25:68–74. <https://doi.org/10.1080/02827581.2010.485819>
- Vogiatzakis IN, Griffiths GH, Zomeni M (2020) Incorporating landscape character in cork oak forest expansion in Sardinia: constraint or opportunity? *Forests* 11:593
- Wang Q, Chu D, Luo C, Lai Z, Shang S, Rahimi S, Mu J (2022) Transformation mechanism from cork into honeycomb-like biochar with rich hierarchical pore structure during slow pyrolysis. *Ind Crop Prod* 181:114827. <https://doi.org/10.1016/j.indcrop.2022.114827>

**Publisher's Note** Springer Nature remains neutral with regard to jurisdictional claims in published maps and institutional affiliations.